Dynamic Air Traffic Flow Coordination for Flow-centric Airspace Management

Chunyao Ma, Sameer Alam, Qing Cai, Daniel Delahaye

▶ **To cite this version:**

Chunyao Ma, Sameer Alam, Qing Cai, Daniel Delahaye. Dynamic Air Traffic Flow Coordination for Flow-centric Airspace Management. USA-Europe ATM Seminar, FAA-Eurocontrol, Jun 2023, Savannah GA, United States. hal-04119152

HAL Id: hal-04119152
https://enac.hal.science/hal-04119152

Submitted on 6 Jun 2023

HAL is a multi-disciplinary open access archive for the deposit and dissemination of scientific research documents, whether they are published or not. The documents may come from teaching and research institutions in France or abroad, or from public or private research centers.

L'archive ouverte pluridisciplinaire **HAL**, est destinée au dépôt et à la diffusion de documents scientifiques de niveau recherche, publiés ou non, émanant des établissements d'enseignement et de recherche français ou étrangers, des laboratoires publics ou privés.

Dynamic Air Traffic Flow Coordination for Flow-centric Airspace Management

Chunyao Ma*, Sameer Alam*, Qing Cai*, Daniel Delahaye†
*Air Traffic Management Research Institute, School of Mechanical and Aerospace Engineering
Nanyang Technological University, Singapore
†OPTIM Lab, Ecole Nationale de l'Aviation Civile, Toulouse, France
Email: *M180146@e.ntu.edu.sg, {*sameeralam| *qcai}@ntu.edu.sg,
†daniel.delahaye@enac.fr

***Abstract*—The air traffic control paradigm is shifting from sector-based operations to cross-border flow-centric approaches to overcome sectors' geographical limits. Under this paradigm, effective air traffic flow coordination at flow intersections is crucial for efficiently utilizing available airspace resources and avoiding inefficiencies caused by high demand. This paper proposes a dynamic air traffic flow coordination framework to identify, predict, assess, and coordinate the evolving air traffic flows to enable more efficient flow configuration. Firstly, nominal flow intersections (NFI) are identified through hierarchical clustering of flight trajectory intersections and graph analytics of daily traffic flow patterns. Secondly, spatial-temporal flow features are represented as sequences of flights transiting through the NFIs over time. These features are used to predict the traffic demand at the NFIs during a given future period through a transformer-based neural network. Thirdly, for each NFI, the acceptable flow limit is determined by identifying the phase transition of the normalized flight transition duration from its neighboring NFIs versus the traffic demand. Finally, when the predicted demand exceeds the flow limit, by evaluating the available capacity at different NFIs in the airspace, the flow excess is alternated onto other NFIs to optimize and re-configure the air traffic demand to avoid traffic overload. An experimental study was carried out in French airspace using the proposed framework base on the ADS-B data in December 2019. Results showed that the proposed prediction model approximated the actual flow values with the coefficient of determination (R^2) above 0.9 and mean absolute percentage error (MAPE) below 20%. Acceptable flow limit determination showed that for above 68% NFIs, the flight transition duration increases sharply when the demand exceeds a certain level. The flow excess at an NFI whose demand was predicted to exceed its limit was coordinated, and the potential increase in the flight transition duration caused by the flow excess was avoided.**

***Index Terms*—air traffic flow coordination, flow-centric operation, air traffic flow prediction, transformer neural networks.**

I. Introduction

The scalability limit of traditional sector-based Air Traffic Control (ATC) services, i.e., difficulty in subdividing heavily loaded sectors, is becoming a barrier to the sustainable growth of air traffic [1]. Researchers have started examining and testing the concept of sectorless ATC, which views the airspace as a whole instead of the current practice of dividing the airspace into small sectors. One primary practice of sectorless airspace is flow-centric operation [2], which relies on controlling and monitoring flow-based formation and evolution of air traffic, i.e., the management of dynamic flow corridors [3]. It opens the opportunity to distribute air traffic more efficiently in the airspace without being constrained by sector boundaries [4].

Despite the benefits of the flow-centric concept, its implementation has been limited. One primary challenge is the efficient coordination of air traffic flow at the intersections to avoid inefficiencies that may jeopardize flight safety [5]. Research focusing on the traditional sector-based air traffic coordination, such as sector traffic prediction and flow optimization for workload balancing between sectors [6], no longer adapts the flow-centric operations where coordination is primarily used to avoid potential inefficiencies or conflicts between the intersecting air traffic flows [4]. Therefore, for safe and efficient airspace management under flow-centric operations, it is crucial to develop a flow-centric-based air traffic coordination framework that can dynamically coordinate air traffic flow in advance based on the collaborative identification, prediction, and inefficiency assessment of the evolving air traffic flows. For instance, traffic flow can be re-routed in advance when the predicted flow demand exceeds the acceptable flow limit at the intersections [4].

Effective air traffic flow identification is the cornerstone for flow-centric-based practices regarding traffic flow analysis, prediction, and coordination [5]. In the literature, air traffic flow has been identified and described in accordance with the airspace configuration, such as the behaviors of groups of flights transiting through area control centers [7], waypoints [8], sectors [9], and airways [10]. Such a characterization of air traffic flow serves the traditional air traffic operations where air traffic control units are geographical sectors and flights have to fly along airways consisting of a set of fixed waypoints. However, flow-centric air traffic management focuses on the flow of air traffic in the airspace from a holistic view disregarding the fixed airways and sectors. It requires air traffic flow identification methods to explore the underlying flow patterns, such as the spatial-temporal evolution of flow locations and structures [11].

In addition to air traffic flow identification, effective air traffic flow coordination requires the constant viewing of air traffic demand according to the available capacity at the flow intersections. Air traffic flow prediction models in the literature primarily take the time series information of the number of flights

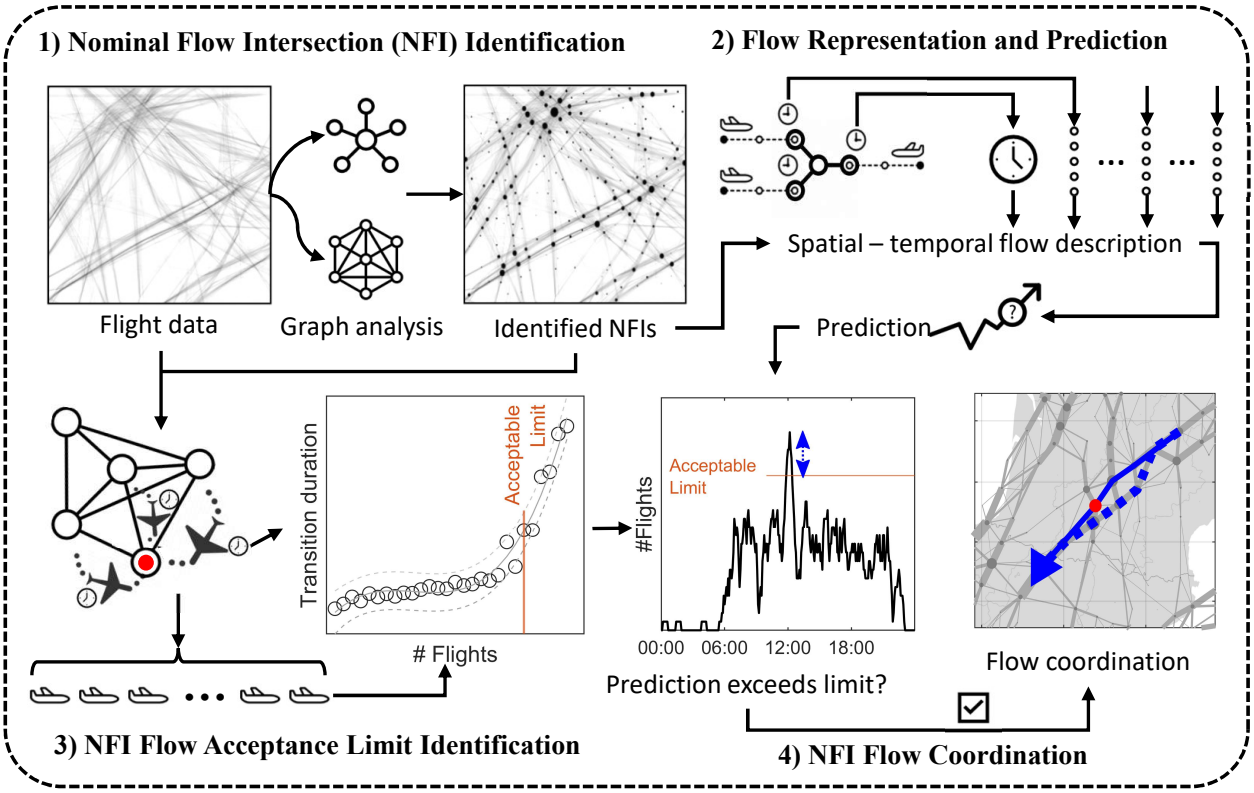

Fig. 1: Conceptual diagram of the proposed dynamic air traffic flow coordination framework, including: 1) NFI identification through graph analysis of air traffic flow patterns; 2) flow representation and prediction based on the spatial-temporal flow distribution; 3) NFI flow acceptance limit identification through flow transition efficiency analysis; 4) Flow coordination, i.e., flow-excess re-routing, based on the capacity availability and predicted flow demand at the NFIs.

at single or multiple geographical locations in the airspace as the input and predict the future number of flights through Linear Dynamic System Models (LDSM) or neural networks such as Long Short-Term Memory (LSTM) [12] and Convolutional Neural Networks (CNNs) [13]. Such time-series-based methods mainly predict future traffic demand by analyzing the past time series [14]. Important spatial-temporal flow dynamics were not incorporated, limiting the modeling and prediction accuracy, which is critical for flow-centric operations where real-time decision-making based on accurate data is necessary. Moreover, the traditional sector-based capacity estimation method lacks consideration of the air traffic flow features, such as the Monitor Alert Parameter(MAP) model regarding the hand-off service workload [15] and the sector merge/split-based model [1]. Therefore, developing flow prediction and acceptance limit identification methods at the flow intersections concerning the evolving flow features is the building block for flow-centric operations.

Information on future air traffic demand and the corresponding acceptable flow limit at the flow intersections enables reconfiguring the air traffic demand transiting through the flow intersections in advance so that air traffic flow can be restricted within a level that does not overload the system excessively [16]. In traditional sectors, air traffic overload is managed by sector operations such as merging and splitting [17]. Under the flow-centric paradigm, traffic flow density and complexity change over time, rendering static flow control operations underloaded or overloaded during the day. Analogically, dynamic flow coordination according to the evolving airspace conditions, such as traffic flow merge/split/re-routing, gives flow-centric airspace an option to address the anticipated flow excess without compromising the flow demand and overloading the acceptable limit at the flow intersections. Therefore, developing dynamic flow coordination algorithms depending on the time-varying traffic flows is an important enabler of efficient flow management decisions and optimal utilization of airspace resources.

In view of the above analysis, this paper proposes a dynamic air traffic flow coordination framework to identify, predict, assess, and coordinate the evolving air traffic flows to enable more efficient flow-centric airspace management. Firstly, nominal flow intersections (NFI) are identified through hierarchical clustering of flight trajectory intersections and graph analytics of daily traffic flow patterns. Secondly, based on the identified NFIs, spatial-temporal flow features are represented as sequences of flights transiting through the NFIs over time. These features are used to predict the future traffic demand at the NFIs through a transformer-based neural network. Thirdly, for each NFI, the acceptable flow limit is determined by identifying the phase transition of the normalized flight transition duration from its neighboring NFIs versus the traffic demand during different periods. Finally, when the predicted future flow exceeds the flow limit, by evaluating the available capacity at different NFIs, the flow excess is alternated onto other NFIs to re-configure the air traffic demand to avoid traffic overload at the NFIs.

II. Problem Description

This paper focuses on the problem of dynamic air traffic flow coordination at the Nominal Flow Intersections (NFIs) for efficient Flow-centric Airspace Management. This problem can be further decomposed into four sub-problems as shown in Fig. 1: 1) identification of NFIs through graph analysis of air traffic flow patterns; 2) flow representation and prediction based on the spatial and temporal dynamics feature of air traffic flows at the NFIs; 3) flow acceptance limit identification at the NFIs through flow transition efficiency analysis; 4) Flow coordination, i.e., flow-excess re-routing, based on the capacity availability and predicted flow demand at the NFIs.

1) NFI Identification: Given the freedom of airspace users taking direct or user-preferred flight routes, one may argue that flow-centric implies insignificant spatial structure and temporal patterns of the air traffic flow. However, taking into account that all flights have to depart and land at airports, the positions of the airports and the scheduled flights between airports restrict the air traffic to an appropriate pattern of main flows. A traffic flow analysis of French airspace, where the free route airspace (a potential coupled working method to flow-centric operations) has been implemented in nearly 50% of the airspace above flight level 195, shows that the majority of flight trajectories are aggregated as major flows connecting major traffic hubs [18]. Thus, the first sub-problem is identifying the locations and the flow inter-connections of the NFIs through constructing and analysing spatial and temporal patterns of air traffic flows.

2) Flow Representation and Prediction: Most existing methods in the literature represent the spatial-temporal air traffic flow features as a time series of the number of flights at different locations without considering the spatial and temporal dynamics feature within the air traffic flow, such as the spatial and temporal distributions of flights in the airspace. The spatial distribution of flights is vital for determining the air traffic complexity and density, while the temporal distribution is essential for describing the dynamic evolution of air traffic [19]. They are the primary influencing factors of the future air traffic at the NFIs, without which the prediction model may fail to learn the causal relations between the input air traffic feature and the prediction target, limiting the model's accuracy in predicting future air traffic flows. Therefore, the second sub-problem is the representation of the spatial-temporal flight distribution and accurate prediction of the future number of flights transiting through the NFIs.

3) NFI Flow Acceptance Limit Identification: Due to the increasing demand for air travel, an NFI may be overloaded by excessive air traffic flows to be coordinated. In a traditional sector-based ATC system, the sector capacity is usually quantified as the maximum number of flights that may enter a sector per hour averaged over a sustainable period and is used to manage a safe, orderly, and efficient traffic flow [20]. Similarly, in flow-centric ATC systems, if the demand at an NFI exceeds an acceptable limit, the efficiencies of air traffic flow transiting through the NFI can be degraded. When an NFI is overloaded, air traffic congestion can be induced, and it will take a longer time for air traffic transiting to the overloaded NFI on the flight paths due to regulatory measures such as vectoring and speed control [21]. Therefore, the third sub-problem is to identify a flow acceptance limit at each NFI above which extra traffic demand will degrade the flow transition efficiency, i.e., the flight transition duration from neighboring NFIs, to the NFI significantly.

4) NFI Flow Coordination: Through solving the above three sub-problems, the locations, the inter-connectivity, the future traffic demand, and the flow acceptance limit of the NFIs can be determined. With this information in hand, the fourth sub-problem is to come up with a flow-centric air traffic excess re-routing algorithm in advance to re-configure the air traffic demand transiting through the NFIs, i.e., re-routing the excessive air traffic flow onto NFIs with spare flow acceptance capability, to avoid exceeding the flow acceptance limit at the NFIs which can cause inefficiencies.

III. Methodology

A. NFI Identification

This paper identifies the NFIs based on the flight trajectories analysis using ADS-B data, including intersection points clustering, daily flow pattern representation, and graph analysis.

1) Intersection Points clustering & Flow Pattern Representation: The NFIs in this paper are defined as the positions in the airspace where air traffic flows intersect. This paper proposes to determine the NFIs by clustering the intersection points of flight trajectories to extract the natural groupings of the intersection points. Hierarchical clustering relies on the hierarchical decomposition of the data based on group similarities to find a multilevel hierarchy of clusters, where clusters at one level are joined as clusters at the next level [22]. Air transportation networks are commonly a nodal hierarchy that follows the spoke–hub structure in which air traffic flows range from regional feeders to international hubs [23]. Therefore, this paper adopts the hierarchical clustering algorithm to discover the NFIs for flow representation.

To determine the optimal number of clusters that should be identified by the clustering algorithm, this paper proposes to model the daily air traffic flow patterns as graphs based on the clustering outcome. The constructed graphs across different days are further investigated and compared to determine the best-fitted number of NFIs for flow pattern representation. The daily air traffic flow pattern is represented as a weighted graph $G = (V, E)$, where V is the set of nodes denoting the air traffic flow components, i.e., the NFIs. The flow connectivity between the nodes can be described by the weighted edges E. The weight of each edge is quantified as the air traffic volume transiting through it, i.e., the number of flights whose trajectories consecutively cross the two nodes connected by the edge.

2) Graph Analysis: The consistent and dependable performance of airspace users is an essential requirement for improving ATM system predictability [24]. Therefore, the representation of traffic flow patterns should describe the behavioral consistency

of air traffic flows in the airspace even though there are daily alternations in the geographical positions of the NFIs and the traffic flow connectivity between NFIs. Under this consideration, this section proposes to determine the optimal number of clusters by modeling and analyzing the consistency of daily flow patterns versus the changes in the number of clusters. The flow pattern consistency is evaluated from two perspectives: a) geographical consistency in node (NFI) locations; b) structural consistency in flow connectivity.

a) Geographical Consistency in NFI locations: To measure the geographical consistency in the daily node locations, a nearest neighbor-based analysis is conducted to match the nodes on the temporal horizon. Given a number of n nodes in the graph G_k constructed for day D_k, let $V_k = \{v_k^1, v_k^2, ..., v_k^i, ..., v_k^n\}$ represent the set of nodes. Similarly, let $V_{k+1} = \{v_{k+1}^1, v_{k+1}^2, ..., v_{k+1}^j, ..., v_{k+1}^n\}$ represent the set of nodes in the graph G_{k+1} constructed for day D_{k+1}. For each node v_k^i in V_k, the proposed algorithm searches for its nearest node $v_{k+1}^{a_i}$ in V_{k+1}. a_i is the index of the identified nearest node of v_k^i in V_{k+1}. By representing node v_k^i's latitude and longitude as $(\varphi_k^i, \lambda_k^i)$ and node v_{k+1}^i's as $(\varphi_{k+1}^i, \lambda_{k+1}^i)$, the nearest neighbour of node v_k^i in V_{k+1} is identified according the great circle distance.

Based on the distances, the nearest neighbouring node $v_{k+1}^{a_i}$ of node v_k^i for $i = 1, ..., n$ can be determined. Similarly, the nearest neighbouring node $v_k^{b_j}$ of node v_{k+1}^j for $j = 1, ..., n$ can be determined with the same process. b_j is the index of the identified nearest node of v_{k+1}^j in V_k. Therefore, two sets of matched node pairs between the two graphs can be obtained: $S_1 : (v_k^1, v_{k+1}^{a_1}), (v_k^2, v_{k+1}^{a_2}), ..., (v_k^n, v_{k+1}^{a_n})$ and $S_2 : (v_k^{b_1}, v_{k+1}^1), (v_k^{b_2}, v_{k+1}^2), ..., (v_k^{b_n}, v_{k+1}^n)$. Then, the geographical consistency of node locations is quantified as the number of mutually matched nodes divided by the total number of nodes, which is formulated as $gc_1 = |S_1 \cup S_2|/n$, where $|S_1 \cup S_2|$ represents the number of node pairs in the union of S_1 and S_2. It will be denoted as l in the rest of the paper.

b) Structural Consistency in Flow Connectivity: Upon determining the geographical consistency in NFI locations, the next step is to quantify the structural consistency in the daily air traffic flow connectivity between the NFIs.

Let $S = S_1 \cup S_2$ represent the set of paired nodes from graph G_k and graph G_{k+1} based on NFI location consistency. While $C_k = \{c_k^1, c_k^2, ..., c_k^l\}$ denotes the nodes in S from graph G_k and $C_{k+1} = \{c_{k+1}^1, c_{k+1}^2, ..., c_{k+1}^l\}$ denotes the corresponding paired nodes from G_{k+1}. Let $e_{c_k}^{i_j}$ represent the edge connecting nodes c_k^i and c_k^j and $w_{c_k}^{i_j}$ represent the weight on it. Let W_{c_k} represent the entire set of edge weights $\{w_{c_k}^{1_2}, w_{c_k}^{1_3}, ..., w_{c_k}^{1_j}, ..., w_{c_k}^{1_l}, ..., w_{c_k}^{2_3}, w_{c_k}^{2_4}, ..., w_{c_k}^{2_j}, ..., w_{c_k}^{2_l}, ..., w_{c_k}^{i_(i+1)}, w_{c_k}^{i_(i+2)}, ..., w_{c_k}^{i_j}, ..., w_{c_k}^{i_l}, ..., w_{c_k}^{(l-1)_l}\}$.

The structural consistency in the air traffic flow patterns is measured by the mutual flow connectivity in the two graphs. More specifically, with the set of paired nodes C_k and C_{k+1} from G_k and G_{k+1} respectively, the flow structure consistency is evaluated by the ratio of the mutual flow connections between the graphs characterized by nodes C_k and C_{k+1} compared to the union of flow connections in G_k and G_{k+1}. It is formulated as:

$$gc_2 = \frac{\sum_{i=1}^{l-1}\sum_{j=i+1}^{l} min(w_{c_k}^{i_j}, w_{c_k+1}^{i_j})}{\sum_{i=1}^{n-1}\sum_{j=i+1}^{n}(w_k^{i_j} + w_{k+1}^{i_j})} \quad (1)$$

Fig. 2 shows a diagram of the graph analysis to determine the node (NFI) location and flow structure consistency. The first column of the figure shows the graphs G_1 and G_2 constructed for the air traffic flow on day 1 and day 2, respectively. The second column of the figure shows the enlarged portions of G_1 and G_2. The nodes, i.e., V_1 and V_2, are marked by solid gray circles. The third column of the figure depicts the mutually paired nodes C_1 and C_2 in the node location consistency analysis of graphs G_1 and G_2. C_1 and C_2 are marked by the red solids, and the paired nodes are labeled by the same number. The fourth column of Fig. 2 displays the two sub-graphs of G_1 and G_2 formed by C_1 and C_2. The numbers on the edges are the edge weight W_{c_1} and W_{c_2}. The fifth column of Fig. 2 shows the determination of mutual connections in the two sub-graphs, i.e., $min\{W_{c_1}, W_{c_2}\}$. $min\{W_{c_1}, W_{c_2}\}$ represents taking the smaller value of the weights on the corresponding edges in the two sub-graphs. For instance, on day 1, the weight on the edge connecting nodes 44 and 166 is 380, meaning there are 380 flights transiting through this edge. While on day 2, the edge weight is 416. Thus, the mutual flow connection on this edge during the two days is considered 380. Eventually, the flow structure consistency is calculated by summing up the mutual connections in the two sub-graphs and dividing this value by the total flow connections in G_1 and G_2.

Calculating the geographical consistency gc_1 and the structural consistency gc_2 versus the varying number of clusters, the "saddle point" on the curves can be adopted as the optimal number of clusters for traffic flow representation. Consequently, the NFIs can be determined by hierarchical clustering based on the determined number of clusters.

B. Flow Representation and Prediction

The above section illustrates the methodology for identifying the NFIs which characterize the nominal air traffic flow intersections across different days of traffic. This section will describe the representation of air traffic flow features and the air traffic flow prediction model. This paper proposes to describe air traffic flow dynamics using the spatial-temporal flights distribution in the airspace. More specifically, the traffic flow feature in the airspace is represented as a text paragraph describing the sequences of flights transiting through the NFIs over time. The proposed method for flow feature representation and prediction consists of three steps: trajectory registration, flow dynamics description using spatial-temporal (S–T) flow distribution, and flow prediction at NFIs.

1) Trajectory Registration: With the identified NFIs, a flight trajectory can be represented as a sequence of the NFIs. The objective of trajectory registration is to search for a sequence

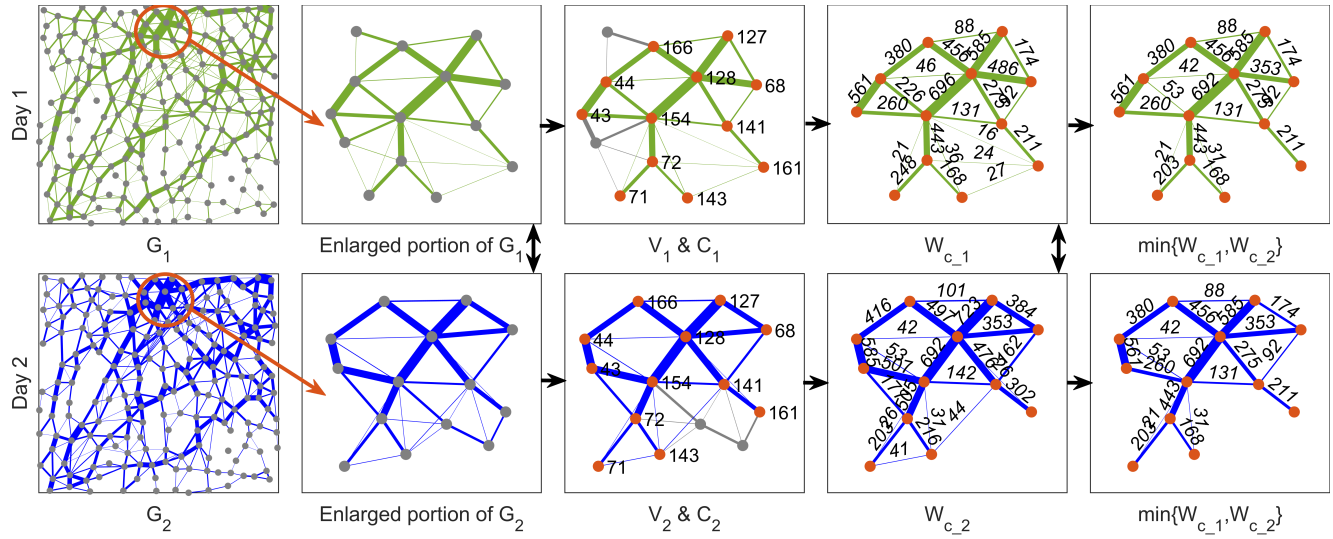

Fig. 2: The diagram for graph analysis of node (NFI) location consistency and flow structure consistency. G_1 and G_2 are the graphs constructed for the air traffic flow on the day 1 and day 2, respectively. The nodes are marked by solid gray circles. The red solids, i.e., C_1 and C_2, in the graphs denote the nodes showing location consistency across the two days. W_{c_1} and W_{c_2} are the edge weights in the two sub-graphs of G_1 and G_2 formed by C_1 and C_2. The structural consistency is characterized by the mutual connections in the two sub-graphs, i.e., $min\{W_{c_1}, W_{c_2}\}$, compared to the total flow connections in G_1 and G_2.

of NFIs that can optimally approximate the original trajectory. This objective is formulated as finding the minimum dissimilarity between the original trajectory and a representative trajectory constituted by a subset of the NFIs. More details regarding the trajectory registration can be found in [18].

2) Flow Dynamics Description Using S–T Flight Distribution: After trajectory registration, we can understand at what time a flight has transited through which NFI. The traffic flow dynamics in the airspace is represented as the spatial-temporal flight distribution, described by "paragraph" whose "sentences" are the sequences of flights transiting through the NFIs. In this paper, a flight is referred to by its callsign. Even though the flight callsign may be changed when airlines introduce updated schedules, in most cases, a flight callsign remains fixed for a particular flight operating on the same route regularly during a relatively long period (such as a season or a few months).

Use t_0 and t_1 to denote the start and end times of a period. Let FP_k denote the traffic flow at NFI v_k during t_0 and t_1. FP_k can be described as a sequence of flights (callsigns) according the time flights passing p_k, i.e., $FP_k : f_k^1, f_k^2, ..., f_k^i, ..., f_k^{m_k}$ with f_k^i denoting the i^{th} flight in the sequence and m_k denoting the total number of flights passing v_k. If there is no flights transited through a NFI, the callsign sequence for this NFI will be replaced by the phrase: "No flights". Analogizing FP_k as a "sentence" depicting the flow context at v_k, the combinations of "sentences" during t_0 and $t_1$constitute a "paragraph" description of the flow context in the entire airspace. The paragraphs for various periods will be used as inputs to the transformer-encoder-based model, introduced in the next section, to learn the contextual relations between air traffic flow and make predictions about the future air traffic flow.

3) Flow Prediction at NFIs: The prediction model is based on the neural network structure developed in by the authors in [18], whose components are tokenization, embedding, transformer encoder blocks, and a fully-connected layer to produce the prediction outcome.

Given an input sequence, i.e., including the time and the flight callsign sequences at the NFIs, word-tokenization [25], which splits the data based on natural breaks and meaning, such as time (number), callsigns (words), and sequence separations (delimiters), is applied to convert the input into a list of integers that can be embedded into a vector space. After tokenization, the token embedding layer converts the list of integers into a list of vectors. For the model to use the order of the elements in the sequence, positional embeddings, which contain information on the relative or absolute position of the elements, are added to the token embeddings as the input to the transformer encoders. The embeddings are trained jointly with the rest of neural network. Back-propagation is carried through all the network layers up to the embeddings that are updated as other parameters. After embedding the elements in the input sequence, each of them flows through the transformer encoder blocks to encode the feature into a meaningful context tensor representation. The transformer encoder is composed of a stack of N_e encoder blocks. The output from the stack of N_e encoders is then forwarded to a fully connected layer to obtain the flow prediction results for different NFIs.

C. NFI Flow Acceptance Limit Identification

To identify the flow acceptance limit at an NFI, this paper proposes to use the flight transition duration from neighboring NFIs as the overload indicator. When the demand at an NFI is above the acceptable limit during a period, air traffic congestion can happen, and it will take a significantly larger time cost for air traffic transiting to the overloaded NFI on their flight paths due to regulatory measures such as vectoring and speed control.

Assume there is a number of N_v NFIs identified, denoted as: $v_1, v_2, ..., v_i, ..., v_{N_v}$. With the time information of flights

reaching the NFIs during the s^{th} period, the number of flights transiting to NFI v_i from NFI v_j can be determined, denoted as n_{ij}^s. The set of transition duration for the n_{ij}^s flights can be denoted as $H_{ij}^s = \{h_{ij}^{s_k} | k = 1, 2, ..., n_{ij}^s\}$, where $h_{ij}^{s_k}$ represents the transition duration of the k^{th} flight among the n_{ij}^s flights. Considering air traffic flows can evolve daily in terms of locations of the NFIs, the traffic flow structure, or unexpected events such as mechanical issues and air traffic control disruptions, the duration H_{ij}^s is normalized by the daily minimum duration to reduce the effects of daily fluctuations in air traffic flow:

$$NH_{ij}^s = \frac{H_{ij}^s}{H_{ij}^{D_s}} \tag{2}$$

where $H_{ij}^{D_s}$ represents the minimum flight transition duration from v_j to v_i on the day of the period s. By doing so for all NFIs that are connected to v_i, the normalized transition duration to v_i for the period s can be obtained: $NH_i^s = \{NH_{ij}^s | j \in N_i\}$, where N_i is the neighbor set of v_i. The total number of flight transiting to v_i can consequently be determined as $n_i^s = \sum n_{ij}^s, j = 1, 2, ..., N_i$.

For all periods $s \in \{1, 2, ..., N_T\}$ in the traffic data, the set of flight transition duration $NH_i = \{NH_i^s | s \in \{1, 2, ..., N_T\}\}$ as well as the set of corresponding traffic demand $n_i = \{n_i^s | s \in \{1, 2, ..., N_T\}\}$ can be determined through the above procedures. By fitting the demand values to the transition duration values, a set of demand values $X = \{1, 2, ..., N\}$ and the corresponding transition duration value $Y = \{y_1, y_2, ..., y_N\}$ can be obtained. The flow acceptance limit is determined by identifying the abrupt changes on the curve of demand versus transition duration, which is formulated as [26]:

$$\begin{aligned} obj = \quad \arg\min_{k} \quad & (k) var([y_1, ..., y_k]) \\ & + (N - k) var([y_{k+1}, ..., y_N]) \end{aligned} \tag{3}$$

By minimizing Eq. 4, the flow acceptance limit l_i at v_i can be determined as k, flow demand above which will lead to abrupt increase in the transition duration of flights to the NFI v_i.

D. NFI Flow Coordination

To re-route the flows at an NFI, a pre-requisite is the knowledge of the main flow paths crossing the NFI, i.e., the main flows transiting through the NFI and their corresponding paths. This paper identifies the main flow paths from the flight data based on the typical sequences of NFIs flown by the flights. Upon identifying the main flows transiting through an NFI, the next step is to predict the number of flights in each main flow during a future period. The prediction model in this step utilizes the same input features and neural network architecture as described in Section III-B, except that the model output is the main flow values at the target NFI instead of the flow demand values of different NFIs.

With the knowledge of the path and predicted demand of each main flow transiting through the NFI, the third step of flow coordination is to re-configure the flow excess by re-routing the main flows so that overload at the NFIs can be avoided. Let f_i represent the predicted flow demand at the NFI v_i. Assume that the predicted flow demand f_* at the NFI v_* exceeds the acceptance limit l_*. Let $\mathbf{A}$ be the adjacency matrix of G, with its entry $a_{ij} = 1$ if NFIs v_i and v_j are connected by traffic flows, otherwise, 0. Given that v_* is predicted to be overload and excessive flow need to be re-routed to the other NFIs, a_{i*} and a_{*j} are set as 0. Assume there is a number of T main flows identified for v_*. Let $D = \{d_1, ..., d_t, ..., d_T\}$ be the vector for the number of re-routed flights in the T flows, i.e., d_t is the number of re-routed flights in the t^{th} flow. Assume that for the t^{th} flow, there are maximum R_t accessible paths respectively denoted by $P_t^1, P_t^2, ..., P_t^r, ..., P_t^{R_t}$. The flow on path P_t^r is represented by f_{tr}. Define a function $\delta_{(tr,ij)}$, with $\delta_{(tr,ij)} = 1$ if the link between v_i and v_j is on the path P_t^r, otherwise, $\delta_{(tr,ij)} = 0$. Let d_{ij} and x_{ij} represent the great circle distance and the amount of flow between v_i and v_j respectively. With all the above notations and definitions, the flow coordination model is formulated as:

$$\begin{aligned} obj = \quad \min_{\substack{\mathbf{X}=\{x_{ij}\} \\ i,j=1,...,N_v}} \quad & \sum_{i=1}^{N_v} \sum_{j=1}^{N_v} a_{ij} x_{ij} d_{ij} \\ s.t. \quad & f_{tr} \geq 0 \\ & \sum_{r=1}^{R_t} f_{tr} = d_t \\ & \sum_{t=1}^{T} d_t = l_* - f_* \\ & \sum_{j=1}^{N_v} a_{ij} x_{ij} \leq l_i - f_i \\ & \sum_{t=1}^{T} \sum_{r=1}^{R_t} \delta(tr, ij) f_{tr} = x_{ij} \end{aligned} \tag{4}$$

Optimizing the above function allows the traffic flow excess at v_* to be re-routed so that minimum flight distance is occurred without exceeding the acceptance limit of all the NFIs.

IV. Experimental Study

To verify the efficacy of the proposed framework, an experimental study has been carried out on the French airspace using one-month ADS-B data from December 1 to December 31, 2019, including a number of 158856 flights. This study focuses on the en-route air traffic above 10,000 ft. The target in this experimental study is set as follows: identify the flow acceptance limits on the NFIs during a 30-minute interval, predict the number of flights that will transit through the NFIs in the future 30 minutes, and re-route the flow excess to avoid overloading the NFIs.

A. NFI Identification

By finding intersections of flight trajectories in the French airspace and clustering the intersection on a daily basis, a graph representation of the daily air traffic flow pattern can be obtained.

By calculating the geographical consistency gc_1 and the structural consistency gc_2 against a set of different cluster numbers ranging from 100 to 1500. A "saddle point" is observed for gc_1 and gc_2 around cluster number 605. Therefore, this paper takes the value 605 as the number of clusters to be identified by

the hierarchical clustering algorithm. The centers of identified clusters are determined as the NFIs.

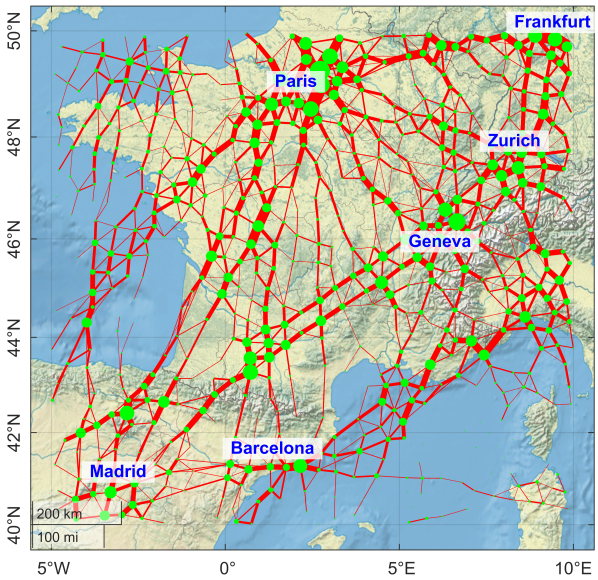

Fig. 3: Graph representation for the one-month air traffic flow using 605 NFIs.

Fig. 3 shows the graph representation for the one-month air traffic structure with 605 NFIs. We can see that this graph is able to depict the nodal hierarchy of air traffic flows ranging from regional feeders to international hubs, such as Paris and Geneva. The en-route air traffic flows are organized as a series of "spokes" connecting the traffic hubs or connecting outlying areas to a hub area.

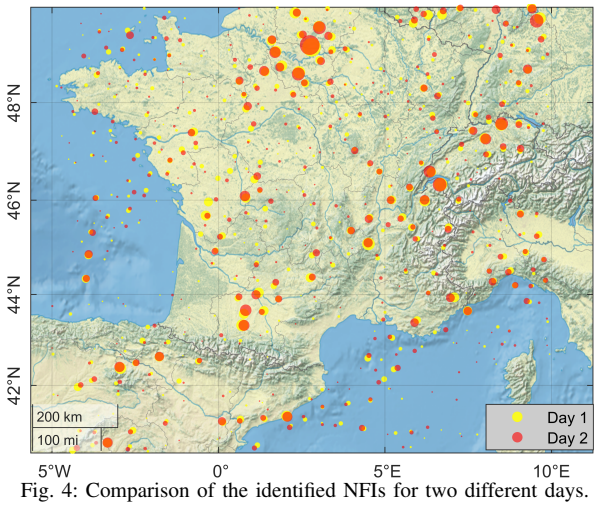

Fig. 4: Comparison of the identified NFIs for two different days.

Fig. 3 presents the NFIs from a spatial structural perspective, and Fig. 4 depicts the temporal dynamics in the NFIs in describing air traffic flows during different days. Fig. 4 shows the identified NFIs for two days, yellow dots for day one and red dots for day two. The dots' sizes are proportional to the traffic volume transiting through the corresponding NFIs. It can be observed that the NFIs show consistent patterns in geographical distribution and traffic volume across different days, although there are some alternations due to the differences in daily air traffic flow organizations.

B. NFI Flow Acceptance Limit Identification

Upon identifying the NFIs and calculating the flight transition duration to the NFIs during different periods and under different traffic flow demand, the flow acceptance limit can be identified by observing the point of demand above which the flight transition durations increases sharply.

Fig. 5 shows the curves of flight transition duration versus the flow demand on eight example NFIs. The blue circles show the original observations obtained from the traffic data, the solid red lines show the fitted curves of the observations, and the pink dashes bound the 95% confidence intervals of the fitting. The curves of duration-demand are fitted using third-degree polynomials. The solid black line indicates the identified acceptance limit of the NFIs. Such phase transitions are observed on 68% of the NFIs, while the transition durations to the rest of the NFIs show no explicit trend concerning the flow demand based on the observations from the one-month data. The reason may be that traffic flow demand on these NFIs is below capacity during this month, so there are no observations for their overloaded circumstances. The flow acceptance limits on such NFIs are set as the maximum flow demand observed.

C. Air Traffic Flow Prediction

After determining the NFIs, the next step will be flow prediction on the NFIs. The prediction model input is the flight callsign sequences on the identified NFIs during the past 30 minutes. The model output is the number of flights transiting through the NFIs in the future 30 minutes.

The prediction model in this study adopts a stack of 12 transformer encoder blocks. The Mean Square Error (MSE) between the predicted and the true values are used to compute the model's loss function. The number of trainable parameters is at the level of 10^8. The training batch size is 16, and the learning rate is 0.00002. The training, test, and validation data consist of 60%, 20%, and 20% of the whole dataset. Concretely, eighteen days of data are used for model training, the following six days of data for model testing, and the last six days for validation.

Fig. 6 presents the traffic flow prediction result on eight example NFIs in the airspace from 00:00 to 23:59 on Dec 24, 2019. The solid blue lines show the true number of flights passing the NFIs, while the red lines show the predicted value using the proposed prediction method. We can observe from Fig. 6 that the proposed method sustainably gives forecasts in close proximity to the actual flow value for different NFIs in the future 30-minute horizon. Furthermore, the prediction method can capture sharp changes in the air traffic demand, as can be observed from the figure that when the actual demand increases or decreases abruptly, the prediction model is still able to give a close prediction of the true value. Overall, the proposed prediction model approximates the actual flow values on the identified NFIs with the coefficient of determination (R^2) above 0.9 and mean absolute percentage error (MAPE) below 20%.

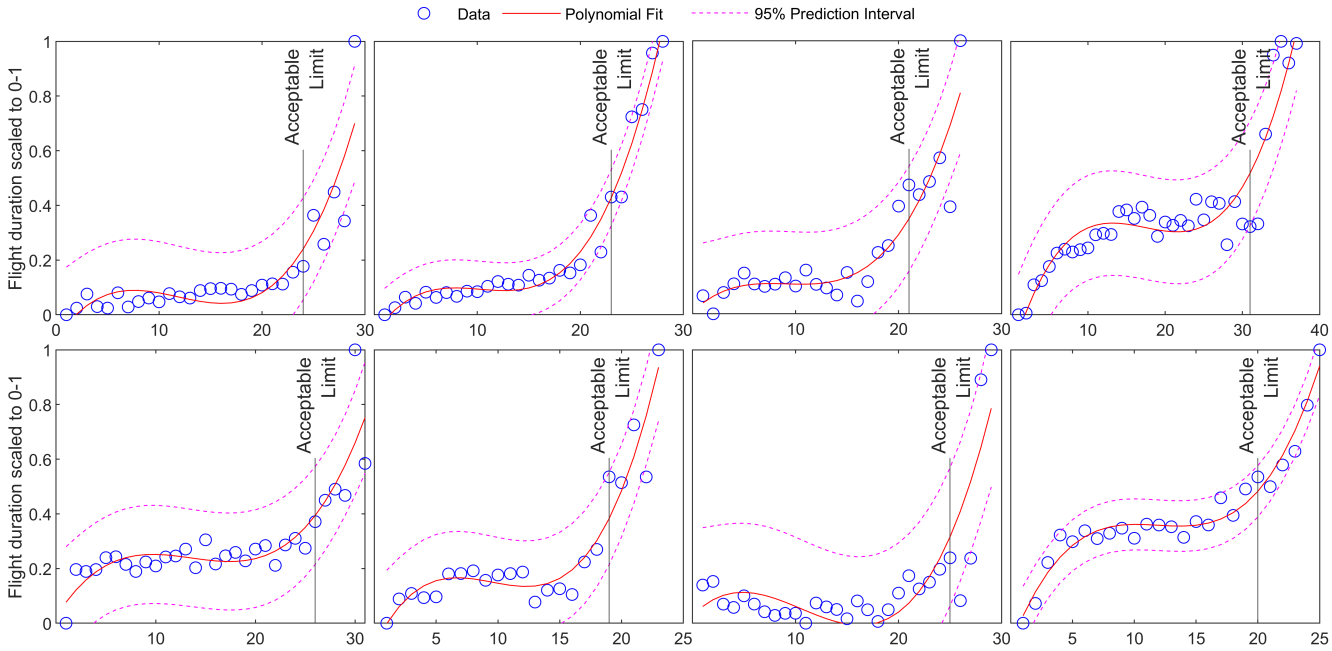

Fig. 5: Flight transition duration versus the flow demand on eight example NFIs. The blue circles show the observations from the traffic data, the solid red lines show the third-degree polynomial fitting of the observations, and the pink dashes bound the 95% confidence intervals of the fitting. The solid black line indicates the identified acceptance limit of the NFIs.

D. NFI Flow Excess Re-routing

Based on the identified flow acceptance limit and the predicted flow during the 30-minute interval, we can observe when an NFI is overloaded and what the flow excess is. It can be observed from Fig. 6 that, for the NFI whose prediction and acceptable flow limit are shown on the bottom-left, the flow is predicted to exceed the acceptable limit from 12:10 to 12:40 on the day. The value of the flow excess is five, meaning five flights should be re-routed to avoid overloading the NFI. This NFI is shown in Fig. 7 and marked by the red node. Three main flows are transiting through the NFI. The green, black, and blue lines visualize the flight trajectories in the three main flows. The predicted flights in the three main flows $t = 1$, $t = 2$, and $t = 3$, are 5, 4, and 8, respectively.

With the knowledge of the number of predicted demand, $f_* = 23$, the acceptable flow limit, $l_* = 18$, and the number of flights in each main flow, this step will re-route the traffic in the main flows onto alternative routes consisting of other NFIs with spare capacity. Although exceptions exist due to traffic congestion or weather conditions, flights in the en-route phase usually prefer the routes with shorter flight distance due to fuel consumption and en-route charges [27]. Therefore, the alternative paths of each main flow, i.e., $P_t^r, for\ t = 1, 2, 3$ in this experiment are set as the two shortest paths, i.e., $R_t = 2, for\ t = 1, 2, 3$ between its origin NFI and destination NFI without transiting through the overloaded NFI. The paths are identified based on the connectivity among the NFIs of the main flow.

Therefore, in this case the Eq. 4 can be specified as follows:

TABLE I. Flow excess re-routing result.

flow	before		f_{t1}	f_{t2}	d_t	after	
	f_{t0}	excess				f_{t0}	excess
$t = 1$	5	5	0	0	0	5	0
$t = 2$	4		0	0	0	4	
$t = 3$	8		5	0	5	3	

$$
\begin{aligned}
obj = \min_{\substack{\mathbf{x}=\{x_{ij}\} \\ i,j=1,\ldots,605}} \quad & \sum_{i=1}^{605}\sum_{j=1}^{605} a_{ij}x_{ij}d_{ij} \\
s.t. \quad & f_{tr} \geq 0 \\
& \textstyle\sum_{r=1}^{2} f_{tr} = d_t \\
& \textstyle\sum_{t=1}^{3} d_t = 5 \\
& \textstyle\sum_{j=1}^{605} a_{ij}x_{ij} \leq l_i - f_i \\
& \textstyle\sum_{t=1}^{3}\sum_{r=1}^{2} \delta(tr, ij) f_{tr} = x_{ij}
\end{aligned}
\tag{5}
$$

Fig. 8 and Table I show the flow excess re-routing result. Five flights in the third main flow marked by solid blue lines are re-routed to its shortest alternative path, i.e., $f_3^1 = 5$, shown by the blue dashes. Note that the predicted demand is 23, and the flow limit is 18. The normalized flight transition duration, scaled between 0 and 1, to the NFI under a demand of 18 flights is 0.27, while under a demand of 23 is 1. Thus, the five flight excess in the traffic flow can potentially lead to a 270% increase in the flight transition duration. Through re-configuring the flow demand at the NFIs, the excess is reduced to 0 from 5, and the anticipated flow overload at the NFI is avoided in advance without causing abrupt increases in the flight durations with the utilization of the spare capacity of other underloaded NFIs.

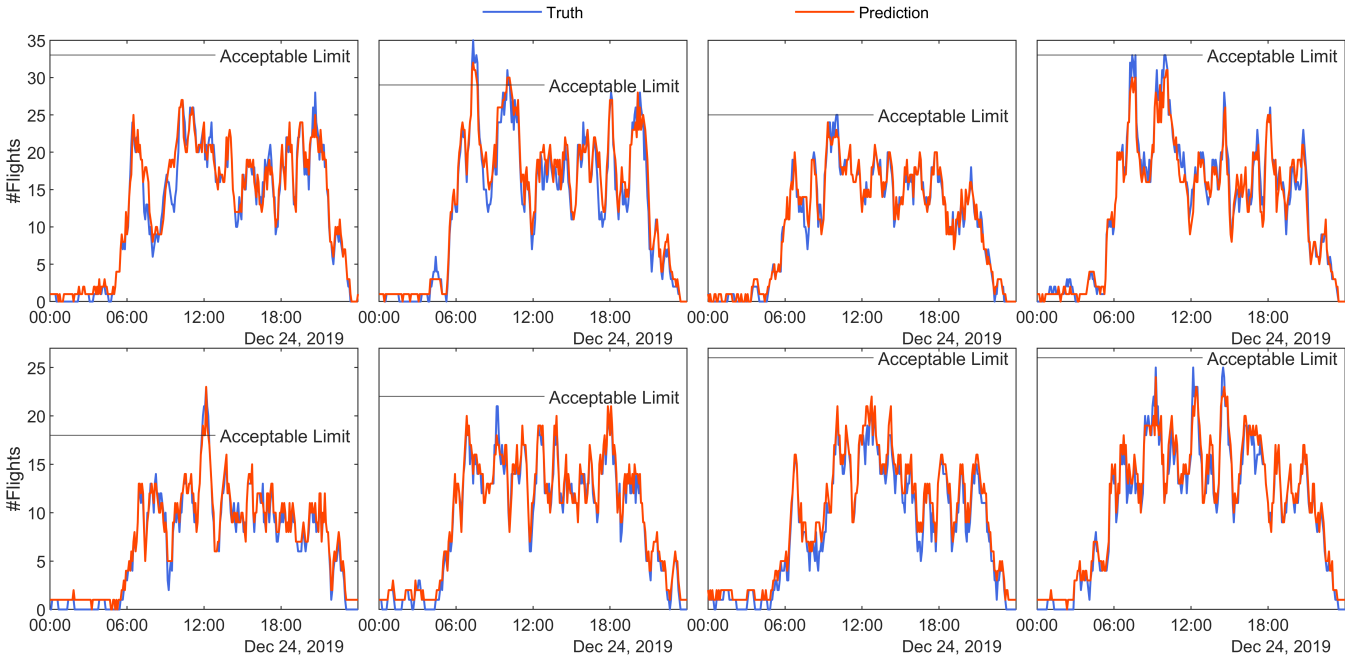

Fig. 6: Flow prediction result on Dec 24, 2019 for eight example NFIs. The solid blue lines show the true number of flights passing the NFIs, while the red lines show the predicted value.

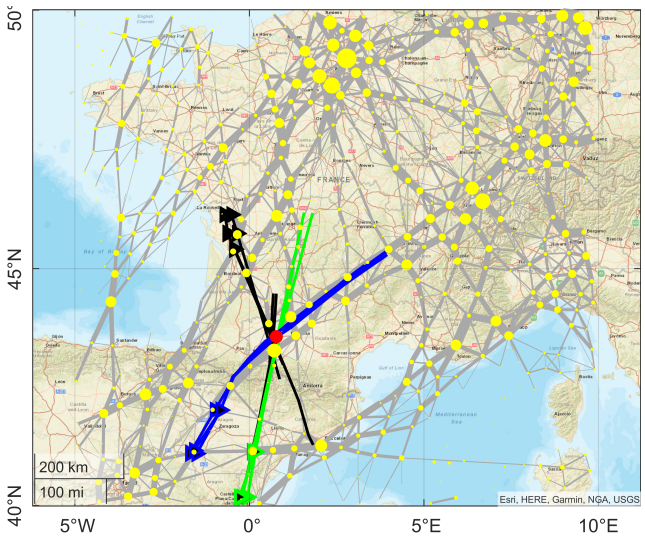

Fig. 7: Three main flows, depicted by the green, blue, and black lines, transiting through the overloaded NFI (red node).

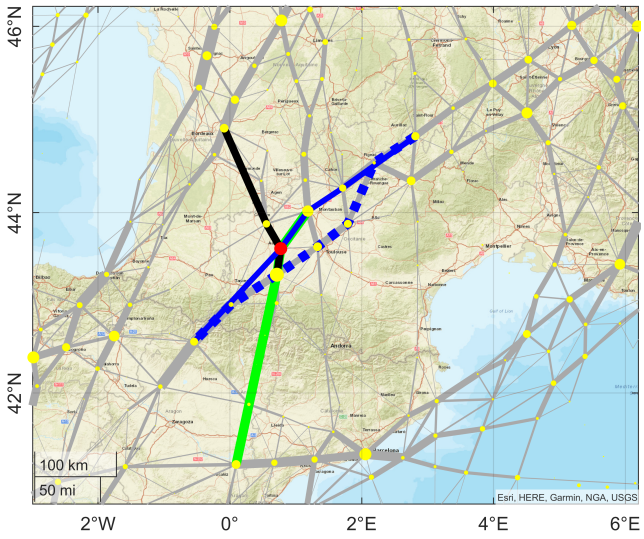

Fig. 8: Flow excess re-routing results. Five flights in the original flow marked by solid blue lines are re-routed to the path shown by the blue dashes.

V. Conclusion and Discussion

Aimed at contributing to the future flow-centric ATC paradigm, which faces challenges in efficiently coordinating air traffic flow at flow intersections, this paper proposed a dynamic air traffic flow coordination framework to identify, predict, assess, and coordinate the evolving air traffic flows. Firstly, nominal flow intersections (NFI) were identified through hierarchical clustering of the flight trajectory intersections. The daily traffic flow patterns were modeled as graphs to determine the optimal number of clusters. A graph analysis was proposed to identify the clustering outcome, which optimally sustained the consistency in the flow patterns. Secondly, based on the identified NFIs, the air traffic flow dynamics features were represented by the spatial-temporal flight distribution, characterized by a textual paragraph recording the time and the sequences of flights passing each NFI. Then, a transformer-based model was adopted to learn the text-enriched flow features and predict future air traffic at the NFIs. Thirdly, for each NFI, the acceptable flow limit was determined by identifying the transition point of

the normalized flight transition duration from its neighboring NFIs versus the traffic demand. Finally, based on the identified acceptable flow limit and the predicted demand, the flow excess at an NFI was alternated onto other NFIs to optimize and re-configure the air traffic demand to avoid sharp increases in flight durations. An experimental study was carried out in French airspace using the proposed framework base on one-month ADS-B data in December 2019. Results showed that the proposed prediction model approximated the actual flow values with the coefficient of determination (R^2) above 0.9 and mean absolute percentage error (MAPE) below 20%. Moreover, acceptable flow limit determination showed that for above 68% NFIs, the flight transition duration increased sharply when the demand exceeded a certain level. Flow overload was avoided by rerouting the detected flow excess to other NFIs with spare capacity.

Research in this paper provides a basic framework for flow-centric air traffic flow coordination. In the future, constraints from both perspectives of air traffic control services and airspace users, such as Special Use Airspace (SUA), weather conditions, airline schedules, and users' preferred routes, can be incorporated to refine this framework for more effective and efficient coordination of air traffic flow. For instance, SUA and weather conditions can be adapted to produce a more accurate and dynamic estimation of the flow acceptance limit. At the same time, airline schedules and users' preferred routes can assist the proposed flow coordination algorithm to re-configure the flow demand to the preferences of airspace users and airlines.

ACKNOWLEDGMENT

This research is supported by the National Research Foundation, Singapore, and the Civil Aviation Authority of Singapore, under the Aviation Transformation Programme. Any opinions, findings and conclusions or recommendations expressed in this material are those of the author(s) and do not reflect the views of National Research Foundation, Singapore and the Civil Aviation Authority of Singapore. The authors would like to thank professor Patric Senac, ENAC, for hosting the first author at ENAC, Toulouse, where part of this research was conducted.

REFERENCES

[1] D. Gianazza, "Learning air traffic controller workload from past sector operations," in *12th USA/Europe Air Traffic Management R&D Seminar, Seattle, United States*, 26-30 June, 2017.

[2] E. Zeki *et al.*, "Business models for flight-centric air traffic control," *Competition and Regulation in Network Industries*, vol. 20, no. 4, pp. 319–332, 2019.

[3] S. Reitmann *et al.*, "Advanced quantification of weather impact on air traffic management," in *ATM Seminar 2019, Vienna, Austria*, 17-21 June, 2019.

[4] S. J. Undertaking *et al.*, "European atm master plan: the roadmap for delivering high performing aviation for europe: executive summary: edition 2015." 2016.

[5] I. Gerdes *et al.*, "From free-route air traffic to an adapted dynamic main-flow system," *Transportation Research Part C: Emerging Technologies*, vol. 115, p. 102633, 2020.

[6] D. Chen *et al.*, "A network based dynamic air traffic flow model for en route airspace system traffic flow optimization," *Transportation Research Part E: Logistics and Transportation Review*, vol. 106, pp. 1–19, 2017.

[7] B. Sridhar *et al.*, "Modeling and optimization in traffic flow management," *Proceedings of the IEEE*, vol. 96, no. 12, pp. 2060–2080, 2008.

[8] M. C. R. Murca and R. J. Hansman, "Identification, characterization, and prediction of traffic flow patterns in multi-airport systems," *IEEE Transactions on Intelligent Transportation Systems*, vol. 20, no. 5, pp. 1683–1696, 2018.

[9] C. Ma *et al.*, "Sector entry flow prediction based on graph convolutional networks," in *International Conference on Research in Air Transportation, Tampa, Florida, USA*, 19-23 June, 2022.

[10] Y. Zhang *et al.*, "A hierarchical heuristic approach for solving air traffic scheduling and routing problem with a novel air traffic model," *IEEE Transactions on Intelligent Transportation Systems*, vol. 20, no. 9, pp. 3421–3434, 2018.

[11] X. Olive and L. Basora, "Identifying anomalies in past en-route trajectories with clustering and anomaly detection methods," in *ATM Seminar 2019, Vienna, Austria*, 17-21 June, 2019.

[12] G. Gui *et al.*, "Machine learning aided air traffic flow analysis based on aviation big data," *IEEE Transactions on Vehicular Technology*, vol. 69, no. 5, pp. 4817–4826, 2020.

[13] Y. Lin *et al.*, "Deep learning based short-term air traffic flow prediction considering temporal–spatial correlation," *Aerospace Science and Technology*, vol. 93, p. 105113, 2019.

[14] R. Dalmau-Codina *et al.*, "A machine learning approach to predict the evolution of air traffic flow management delay," in *2021 ATM Seminar virtual event*, 20-24 Sep 2021.

[15] B. Marr and K. Lindsay, "Controller workload-based calculation of monitor alert parameters for en route sectors," in *15th AIAA Aviation Technology, Integration, and Operations Conference, Dallas, TX*, 22-26 June, 2015, pp. 3178–3188.

[16] Y. Lin *et al.*, "From aircraft tracking data to network delay model: A data-driven approach considering en-route congestion," *Transportation Research Part C: Emerging Technologies*, vol. 131, p. 103329, 2021.

[17] Z. Liu *et al.*, "A framework for strategic online en-route operations: Integrating traffic flow and strategic conflict managements," *Transportation Research Part C: Emerging Technologies*, vol. 147, p. 103996, 2023.

[18] C. Ma *et al.*, "Air traffic flow representation and prediction using transformer in flow-centric airspace," in *SESAR Innovation Days*, 5-8 December, 2022.

[19] D. Delahaye *et al.*, "Air traffic complexity map based on linear dynamical systems," *Aerospace*, vol. 9, no. 5, p. 230, 2022.

[20] J. D. Welch *et al.*, "Sector workload model for benefits analysis and convective weather capacity prediction," in *Tenth USA/Europe Air Traffic Management Research and Development Seminar (ATM2013), Chicago, IL*, 2013.

[21] P. Baumgarten *et al.*, "The impact of hubbing concentration on flight delays within airline networks: An empirical analysis of the us domestic market," *Transportation Research Part E: Logistics and Transportation Review*, vol. 66, pp. 103–114, 2014.

[22] Q. Cai and J. Liu, "Hierarchical clustering of bipartite networks based on multiobjective optimization," *IEEE Transactions on Network Science and Engineering*, vol. 7, no. 1, pp. 421–434, 2018.

[23] F. Seabra *et al.*, "Determinants of brazilian international flights: The role of hub-and-spoke and infrastructure variables," *Journal of Air Transport Management*, vol. 89, p. 101866, 2020.

[24] M. C. R. Murça *et al.*, "Flight trajectory data analytics for characterization of air traffic flows: A comparative analysis of terminal area operations between new york, hong kong and sao paulo," *Transportation Research Part C: Emerging Technologies*, vol. 97, pp. 324–347, 2018.

[25] L. Sun *et al.*, "Spectral–spatial feature tokenization transformer for hyperspectral image classification," *IEEE Transactions on Geoscience and Remote Sensing*, vol. 60, pp. 1–14, 2022.

[26] R. Killick *et al.*, "Optimal detection of changepoints with a linear computational cost," *Journal of the American Statistical Association*, vol. 107, no. 500, pp. 1590–1598, 2012.

[27] M. Soler *et al.*, "En-route optimal flight planning constrained to pass through waypoints using minlp," in *Ninth USA/Europe Air Traffic Management Research and Development Seminar (ATM2011),Berlin, Germany*, June 14-17, 2011.